

Type of the Paper: Original Research

# Evaluation of Iron Ore Dust Emission Rates and Associated Bacterial Load

Melainine Aillal<sup>1</sup>†, Olfa Ben Said<sup>2,3</sup>, Hamouda Beyrem<sup>2</sup> and Zeinebou Sidoumou<sup>1</sup>

<sup>1</sup>University of Nouakchott, Faculty of Science and Technology, New University Campus, 5026, Nouakchott, Mauritania

<sup>2</sup>Laboratory of Environment Biomonitoring, Coastal Ecology Unit, Faculty of Sciences of Bizerte, University of Carthage, Zarzouna, Tunisia

<sup>3</sup>Laboratory of Biotechnology and Nuclear Technology, National Centre of Nuclear Science and Technology, Sidi Thabet Technopark, 2020 Ariana, Tunisia.

†Corresponding author: Melainine Aillal; melainineaillal@gmail.com

Melainine Aillal : ORCID : 0009-0001-5457-4216 ; Olfa Ben Said : ORCID : 0000-0002-1372-5719

Hamouda Beyrem: ORCID : 0000-0003-0738-4257 ; Zeinebou Sidoumou: ORCID : 0000-0002-3680-3046

Key Words	Mining activities, Dust emissions, Heavy metals, Environmental pollution, Staphylococcus, Occupational health.
DOI	<a href="https://doi.org/10.46488/NEPT.2026.v25i04.D1905">https://doi.org/10.46488/NEPT.2026.v25i04.D1905</a> (DOI will be active only after the final publication of the paper)
Citation for the Paper	Aillal, M., Ben Said, O., Beyrem, H. and Sidoumou, Z., 2026. Evaluation of iron ore dust emission rates and associated bacterial load. <i>Nature Environment and Pollution Technology</i> , 25(4), D1905. <a href="https://doi.org/10.46488/NEPT.2026.v25i04.D1905">https://doi.org/10.46488/NEPT.2026.v25i04.D1905</a>

## ABSTRACT

The National Company for Industry and Mines is facing significant dust emissions, raising serious environmental and public health concerns. This study aimed to characterize airborne dust emissions from mining activities and to assess their physicochemical and microbiological composition. Dust samples were analyzed and found to contain hazardous heavy metals, including lead, copper, nickel, and cobalt. A standardized measurement procedure was developed and applied in accordance with French Standard X 43-014 to quantify dust emission rates.

The potential sources and causes of dust emissions were identified, and immediate preventive and corrective actions were proposed using the Failure Modes, Effects, and Criticality Analysis (FMECA) method. The results revealed exceptionally high dust emission levels at the Guelb El Rhein mine, exceeding the thresholds associated with highly polluted environments. In contrast, emissions at the Kedia d'Idjil mine remained close to regulatory limits and were comparable to levels observed in relatively livable environments.

Microbiological analysis of dust particles revealed the presence of potentially pathogenic staphylococcal species, including *Staphylococcus epidermidis*, *S. hominis*, *S. capitis*, *S. haemolyticus*, *S. lentus*, *S. auricularis*, *S. sciuri*, and *S. cohnii subsp. urealyticum*. These findings highlight the combined chemical and biological risks associated with mining dust emissions and underscore the need for improved dust management strategies in mining environments.

## 1. INTRODUCTION

Atmospheric pollution has existed for centuries, but has intensified considerably with the expansion of human activities. The large-scale production of energy through combustion processes and the rapid development of industrial operations have profoundly disrupted natural atmospheric balances, not only at local scales but also globally. These changes have led to significant degradation of air quality and have contributed to climate change (Boussahel 2007). Atmospheric emissions include not only gases and fine particulate matter but also heavy metals and various chemical compounds that can exert toxic effects on ecosystems and human health.

The mechanisms governing environmental contamination through atmospheric deposition remain insufficiently understood. During cloud formation, pollutants are partitioned among different atmospheric phases, namely gaseous, liquid, and particulate. While gas–liquid equilibrium processes have been extensively studied, interactions between particulate and liquid phases are still poorly documented. Recent studies have demonstrated that the pollutant load varies according to particle size, which strongly influences particle transport, deposition processes, and environmental fate (Ma et al. 2014; Hassanvand et al. 2015). Fine particles are capable of long-range transport, whereas coarse particles tend to deposit more rapidly, leading to pronounced local impacts on air, soil, and water quality.

Air pollution remains one of the most critical global environmental challenges and continues to intensify due to rapid urbanization and the expansion of industrial and mining activities. This situation underscores the urgent need to control emissions in order to protect both public health and the environment (Elodie et al. 2020). In addition to chemical contamination, air particularly indoor air in industrial settings can serve as a favorable medium for the development and persistence of pathogenic microorganisms associated with dust and aerosols (Viegas et al. 2020; Yan et al. 2021). Previous research has shown that airborne dust and bioaerosols can significantly increase occupational health risks, including infections, toxic effects, and allergic responses (Eduard et al. 2012; Heederik & Von Mutius 2012).

In Mauritania, the discovery and exploitation of mineral resources over the past two decades have led to the rapid expansion of mining projects, predominantly using open-pit extraction methods. One of the most significant environmental threats associated with these operations is the generation of large quantities of suspended particulate matter, which can adversely affect soils, vegetation, and nearby populations (Antoine 2012). Consequently, mining companies operating in the country are confronted not only with production-related challenges but also with increasing concerns regarding the environmental and health impacts of dust emissions, which have become a major issue for both employers and local authorities.

The National Industrial and Mining Company (SNIM), which specializes in iron ore production, operates mainly in the regions of Tiris Zemour (Zouérate) and Dakhlet Nouadhibou in Mauritania (Fig. 1). Ore extraction and processing activities are primarily conducted near the city of Zouérat, after which the products are transported to Nouadhibou for export. The ore is conveyed over a distance of approximately 700 km by a 2.5 km-long ore train with an average capacity of 17,000 tons per convoy. From Nouadhibou, where SNIM operates two mineral ports, iron ore products are shipped to several Western European countries and China (SNIM 2022).

An Environmental and Social Impact Assessment conducted in 2009 for SNIM mining operations indicated that air pollution associated with the Guelbs 1 facilities posed significant risks to human health, particularly with respect to respiratory diseases. The assessment further predicted that the development of the Guelbs 2 project would increase dust emissions by 10–15% (Tecsult International Limited 2009). According to this study, workers involved in the Guelbs 2 project would be exposed to concentrations of total dust, quartz dust containing silica, iron dust, and welding fumes exceeding applicable regulatory standards, thereby necessitating the implementation of corrective and preventive measures.

In this context, the present study focuses on dust emissions from SNIM's Guelb El Rhein (Guelbs 2) and Kedia d'Idjil (TO14, Rouessa) mining sites, which were selected due to their substantial dust-generating activities. A corrective approach was implemented alongside a detailed assessment of dust emission levels and the associated bacterial load in airborne particles. The objective of this work is to improve understanding of the combined environmental and health impacts of mining-related dust emissions and to contribute to the development of effective mitigation strategies for mining environments.

## 2. MATERIALS AND METHODS

Dust assessment can be conducted using three main approaches: (i) measurement of airborne particulate concentrations (TSP, PM<sub>10</sub>, PM<sub>2.5</sub>), expressed in  $\mu\text{g}/\text{m}^3$  (Winberry 1999); (ii) quantification of deposited dust expressed in  $\text{mg}/\text{m}^2/\text{day}$ , which is the method adopted in this study; and (iii) estimation of total annual emissions expressed in tons per year (t/year), according to particle size fractions.

The quantification method applied in this study is based on dust sampling over a defined exposure period. From a qualitative perspective, several analytical techniques were employed: X-ray fluorescence (XRF) for elemental composition, X-ray diffraction (XRD) for mineralogical characterization and silica content, atomic absorption spectrometry for heavy metal determination, the Most Probable Number (MPN) method for bacterial quantification, and the API gallery system for bacterial species identification (NIOSH 1998).

### 2.1. Quantification of Sedimented Dust ( $\text{mg}/\text{m}^2/\text{day}$ )

The procedure used to measure deposited dust followed the French standard NF X 43-014 (AFNOR 2003), as recommended by INERIS (INERIS 2003). Dust was collected using Bergerhoff or Owen deposit gauges, which were weighed before and after the exposure period. Sampling devices were installed in accordance with standard recommendations, away from high-risk zones and major traffic sources.

The dust monitoring was conducted using Owen gauges, which were strategically positioned at each sampling point at a standardized height of 1.5 m above ground level to minimize the influence of saltating particles from the soil surface. To quantify the atmospheric dust fallout, the total mass of the collected particles was related to the sampling surface and the exposure time. The dust deposition rate ( $T$ ) was calculated according to the following formula:

$$T = \frac{P}{S \times t}$$

Where:

- $T$ : Dust deposition rate ( $\text{mg}/\text{m}^2/\text{day}$ )
- $P$ : Total mass of the dust collected in the gauge (mg)
- $S$ : Surface area of the gauge opening ( $\text{m}^2$ )
- $t$ : Duration of the exposure period (days)

This calculation procedure follows the rigorous recommendations of the NF X 43-014 standard for the measurement of atmospheric dust fallout. This standardized approach ensures that the exceptionally high values recorded at the source-point stations are a precise reflection of the intense industrial activity at the mining sites during the sampling window.

Dust pollution levels were classified as follows:

- Very low: < 150 mg/m<sup>2</sup>/day (low pollution area)
- Low: 150–350 mg/m<sup>2</sup>/day (moderately polluted area)
- High: 350–500 mg/m<sup>2</sup>/day (polluted area)
- Very high: 500–1,000 mg/m<sup>2</sup>/day (highly polluted area)
- Extremely high: > 1,000 mg/m<sup>2</sup>/day (very heavily polluted area) (Budillon Rabatel 2009)

## 2.2. Study Area and Sampling Strategy

The study was conducted at two major mining sites located near Zouérate, northern Mauritania: the Guelb El Rhein magnetite mine and the Kédia d'Idjil hematite mine. Sampling was carried out over two weeks from August 2 to August 16, 2019.

Dust deposition was monitored at six sampling points distributed across the two sites (Fig. 1), including three points along the Guelb 2 production circuit and three points within the Kédia d'Idjil mining area.

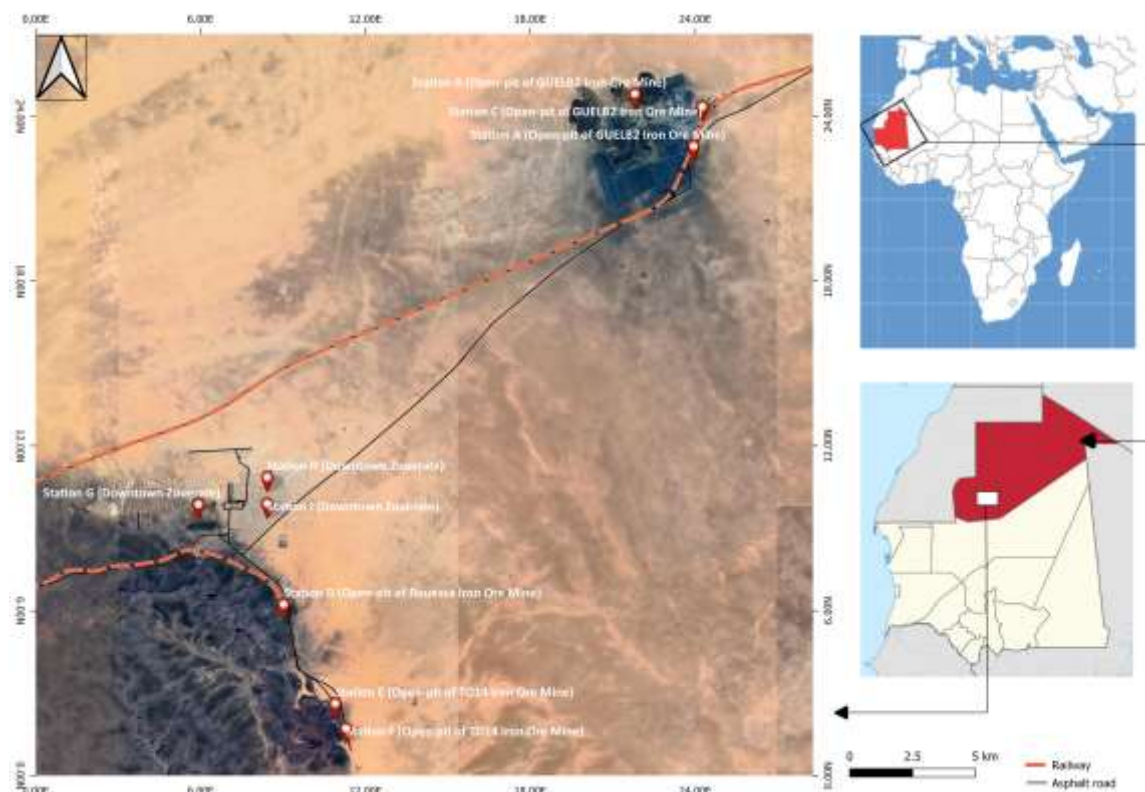


Fig. 1: Location of sampling stations within the National Industrial and Mining Company (SNIM), in the Tiris Zemmour region, Mauritania. Stations A, B, and C are located in the Guelb El Rhein mine, along the production circuit of Guelb 2. Stations D (at Rouessa), E, and F (in the TO14 area) are situated in the Kedia d'Idjil mine. Stations G, H, and I are located in downtown Zouerate.

Climatic conditions during the monitoring period were characterized by temperatures ranging from 22°C to 43°C, absence of precipitation, and wind speeds varying between 12 km/h and 52 km/h (Blanchon & Penven 2012). While the two-week monitoring period (August 2–16, 2019) captures a specific temporal window, it coincides with extreme summer conditions in the Saharan climate, characterized by peak temperatures and significant wind speeds conducive to maximum dust suspension. We acknowledge that this short duration does not account for annual seasonal variability; however, it provides a critical baseline for peak emission periods during the dry season.

### **2.3. Chemical and Mineralogical Analyses**

Elemental composition of dust samples was determined using X-ray fluorescence (XRF), allowing quantification of major oxides including CaO, SiO<sub>2</sub>, MgO, Fe<sub>2</sub>O<sub>3</sub>, Al<sub>2</sub>O<sub>3</sub>, SO<sub>3</sub>, K<sub>2</sub>O, and Na<sub>2</sub>O. XRF analysis enabled continuous monitoring of dust composition throughout the sampling period (Jensen et al. 2006).

Mineralogical composition and crystalline structure were analyzed by X-ray diffractometry (XRD) (Ron 2006).

The exploitation of hematite (Fe<sub>2</sub>O<sub>3</sub>) and magnetite (Fe<sub>3</sub>O<sub>4</sub>) ores constitutes a significant source of heavy metals such as Ni, Pb, Cu, Co, Cd, and Zn. These metals are transported by dust particles and deposited on surrounding surfaces at distances influenced by wind speed and particle size (Simpson & Spadaro 2016, Embile Jr. et al. 2018, Mendes et al. 2018). Elevated iron concentrations commonly observed in polluted mining environments may induce analytical interferences, notably Fe/Cu and Co/Fe interactions (Adamson et al. 2000, Manceau et al. 2002, Sammut 2007, Aillal et al. 2023).

To minimize such interferences, heavy metal analyses were performed on the fine fraction of iron ore dust using Flame Atomic Absorption Spectroscopy (FAAS) following acid digestion with HCl, HF, and HNO<sub>3</sub> (López-García et al. 1995). The metals quantified included Co, Cu, Ni, and Pb (Fig. 5).

### **2.4. Microbiological Analyses**

#### ***2.4.1. Total Cultivable Bacterial Quantification***

For inoculum preparation, dust samples from each sampling site were homogenized, weighed, and stored in sterile screw-capped tubes. For each dust type (magnetite from Guelb El Rhein and hematite from Kédia d'Idjil), 1.5 g of dust was suspended in 5 mL of sterile physiological saline solution. Serial dilutions were prepared using physiological water (9 g/L NaCl) according to the suspension–dilution technique described by Rapilly (1968).

Bacterial enumeration was performed using the Most Probable Number (MPN) method with five-tube series. Tubes were incubated at 37°C for 48 hours. Nutritive broth, thioglycollate medium, and LB broth were used for bacterial growth and quantification (Chandrapati & Williams 2014).

#### **2.4.2. Isolation and Characterization of Anaerobic Bacterial Strains**

Three grams of hematite dust and three grams of magnetite dust were suspended separately in 5 mL of sterile physiological water and subjected to thermal shock at 63°C to eliminate vegetative cells while preserving sporulated forms (Cammalleri et al. 2015). Serial dilutions were prepared, and selected dilutions were inoculated onto iron sulfite agar under anaerobic conditions and incubated at 37°C.

Dominant strains were purified through successive subcultures. Preliminary identification was based on growth on selective media, Gram staining, spore staining, and macroscopic and microscopic observations using standard taxonomic keys.

#### **2.4.3. Identification Using the API Staph System**

Bacterial identification was further performed using the API Staph system, which consists of 19 microtubes containing dehydrated substrates for the differentiation of *Staphylococcus*, *Kocuria*, and *Micrococcus* species (Aouissi et al. 2007; Rouaiguia 2010). The galleries were incubated at 37°C for 24 hours, and biochemical profiles were interpreted according to the manufacturer's instructions (Brown & Smith 2015). Final identification was confirmed using dedicated microbial identification software (Debabza 2015).

### **2.5. Failure Modes, Effects, and Criticality Analysis (FMECA)**

The Failure Modes, Effects, and Criticality Analysis (FMECA), also referred to as AMDEC, is a preventive and inductive method used to identify potential failures and implement corrective actions at an early stage (Kenneth & Gilbert 1980). This approach applies to products, processes, and production systems and is widely used in industrial risk assessment and environmental management (Hariz 2009).

### **2.6. Statistical Analysis**

Dust emission data were expressed as mean  $\pm$  standard deviation (SD). Statistical analyses were performed using STATISTICA version 8 software. Differences between dust emission rates were evaluated using one-way analysis of variance (ANOVA), followed by Tukey's HSD post hoc test when significant differences were observed. Statistical significance was set at  $p < 0.05$ .

## **3. RESULTS**

### 3.1. Results of Dust Emission Rates

Dust emissions occur at different levels of the National Industrial and Mining Company (SNIM). However, this work focuses only on the iron ore production sites of Guelb El Rhein (Guelb 2), Kedia d'Idjil (TO14 and Rouessa), as well as downtown Zouerate. The results of this monitoring and the measurements carried out during the period from August 2 to 16, 2019, are presented in Table 1.

Table 1. Results of the dust emission control of the national industrial and mining company "SNIM" during the period of 2-16 August 2019.

Sites	Gauge location	Owen gauge	Emission rate in mg/m <sup>2</sup> /d
Guelb El Rhein	Guelb 2	A	38045
		B	27901
		C	50480
Kedia D'Idjil	Rouessa	D	19007
	TO14	E	12076
		F	15146
Zouerate	Downtown	G	594
		H	596
		I	592

To have an idea of the variation of these emissions over time, a graphical representation of the average emission rates in each collection site was made (Fig. 2).

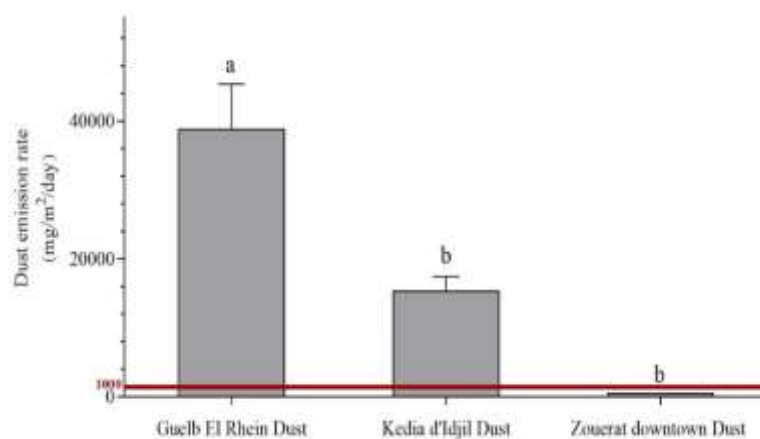


Fig. 2: Graphical representation of the Mean  $\pm$  standard deviation of dust emission rates. The data indicated by different letters are statistically different (Tukey's HSD test:  $p < 0.05$ ).

One-way ANOVA revealed significant differences in dust emission rates between the three main locations (F-statistic,  $p < 0.001$ ). As shown in Fig. 2, post hoc Tukey's HSD tests confirm that the emission rate at Guelb El Rhein is statistically higher than at Kedia d'Idjil and Zouerate ( $p < 0.05$ ), with the latter being significantly the lowest.

### 3.2. Chemical Analysis

The dust collected from two deposits (Ghuelb El Rhein and Kedia d'Idjil) was the subject of a series of chemical analyses carried out by the XRF, XRD, and AAS systems. Fig. 3 shows the results of the X-ray fluorescence (XRF) analyses.

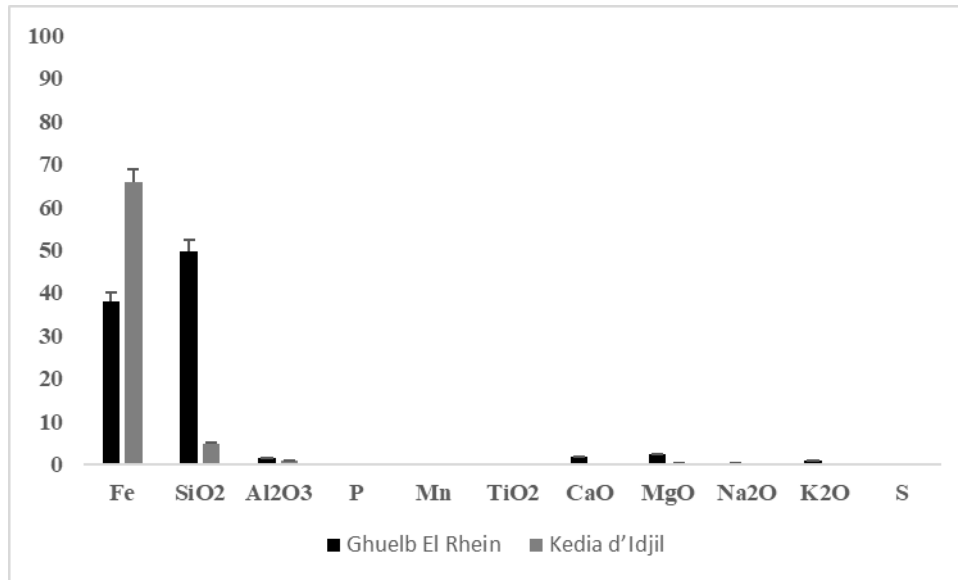


Fig. 3: The graphical representation of the average  $\pm$  standard deviation of percent X-ray fluorescence (XRF) analyses.

The results obtained show that the dust emitted at the level of Guelb El Rhein is 38.1  $\pm$  2.2% iron oxide, which indicates that it is Magnetite type (37% iron content); however, this ore must undergo an enrichment process to reach the commercial value set by the company at 66% Iron. As for the dust obtained at Kedia d'Idjil, the analysis shows a content of 65.7  $\pm$  1.9% iron; this value is relative to the hematite-type ore (66% iron content).

Based on these results, an X-ray diffractometer was used to determine the type of silica in the iron oxide-silica mixture in a fraction approaching the alveolar fraction (Fig. 4).

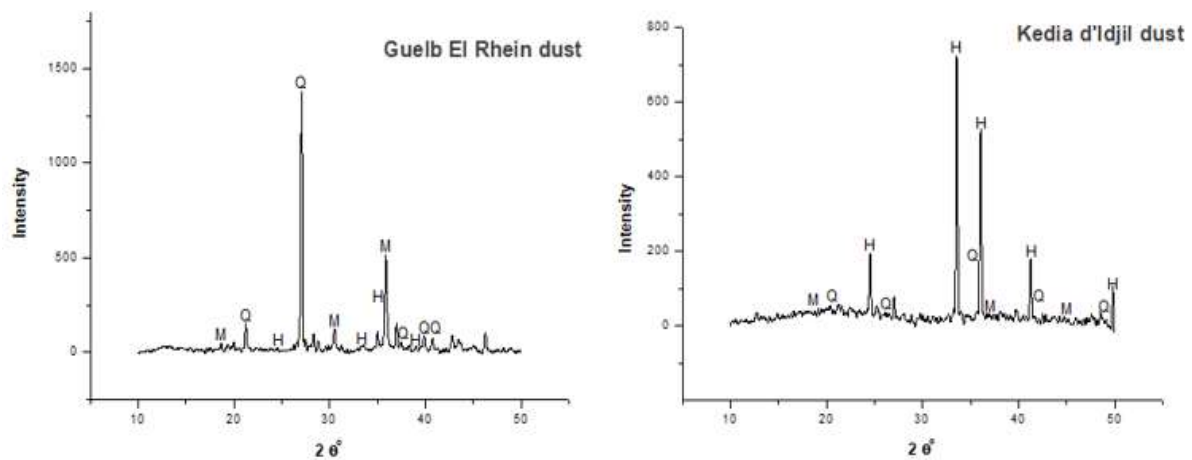


Fig. 4 : X-ray diffraction diagrams for dust samples from Guelb El Rhein and Idjil Kedia. H, hematite; M, magnetite; Q, quartz.

The mineralogical analysis indicates that the iron ore of the national industrial and mining company is composed essentially of hematite ( $\text{Fe}_2\text{O}_3$ ), quartz ( $\text{SiO}_2$ ), and magnetite ( $\text{Fe}_3\text{O}_4$ ).

The diffractogram of the dust emitted by the deposit of Guelb El Rhein reveals mainly the presence of three intense peaks: The peak represented by quartz  $2\theta = 27^\circ$ , the one appearing at  $2\theta = 36^\circ$ , corresponding to magnetites, and the one located at  $2\theta = 35^\circ$ , corresponding to hematite. As for the diffractogram of the dust emitted by the Kedia d'Idjil deposit essentially shows the presence of hematite in five intense peaks, magnetite with weak peaks, and quartz appears at  $2\theta = 35^\circ$  in its best state. The presence of high levels of iron in the dust, as shown in Fig. 3, was widespread in the contaminated sites and can cause significant interferences with heavy metals. Dust samples from Kedia d'Idjil and Guelb El Rhein were analyzed using the SAA-Flame technique (Fig. 5).

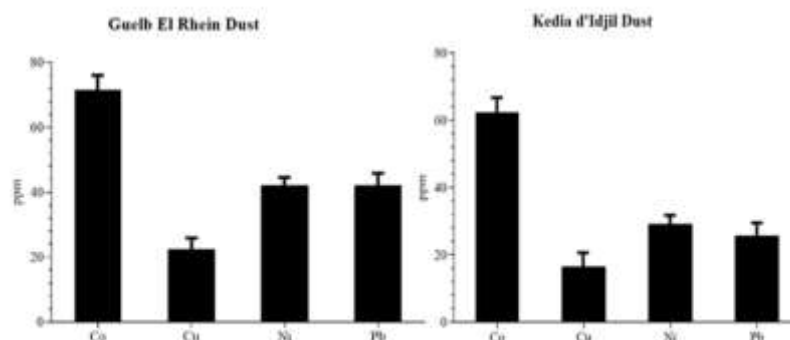


Fig. 5: Heavy metal (Co, Cu, Ni, and Pb) contents measured in the two types of iron ore dust, namely Guelb El Rhein Dust and Kedia d'Idjil Dust.

The primary focus of the study was to assess dust emissions from iron ore extraction, with a particular emphasis on heavy metal concentrations. To this end, representative samples of iron ore dust from Guelb El Rhein and Kedia d'Idjil

were collected and subjected to detailed analysis (Fig. 5). The findings reveal distinct variation in mean levels of heavy metals. The highest peaks belong to cobalt (Co) and the lowest to copper (Cu). Kedia d'Idjil dust samples have average values of 62.42 mg/kg of Co, 16.41 mg/kg of Cu, 29.08 mg/kg of Ni, and 25.71 mg/kg of Pb, respectively. However, the dust samples from Guelb El Rhein have Co, Cu, Ni, and Pb concentrations of 71.62, 22.34, 42.04, and 42.62 mg/kg, respectively. The concentration order for the Kedia d'Idjil samples is  $Co > Ni > Pb > Cu$ , with values of 62.42 mg/kg, 29.08 mg/kg, 25.71 mg/kg, and 16.41 mg/kg. For the Guelb El Rhein samples, the order is  $Co > Pb > Ni > Cu$ , with corresponding values of 71.62 mg/kg, 42.62 mg/kg, 42.04 mg/kg, and 22.34 mg/kg.

Notably, the concentrations of heavy metals in dust samples collected from the city center of Zouerate were below the detection threshold. The concentration of Co (71.62 mg/kg) and Ni (42.04 mg/kg) in Guelb El Rhein dust is notably high when compared to the urban control (Zouerate), where these metals were undetectable. These levels approach or exceed common soil quality guidelines for industrial zones, suggesting that long-term deposition could lead to significant soil enrichment and potential ecological transfer, particularly given the fine fraction's capacity for transport. This study also shows that heavy metal content in the Guelb El Rhein samples of dust is significantly higher than it is for samples from Kedia d'Idjil. This conclusion points the finger at a potentially higher environmental impact of dust emissions in Guelb El Rhein when compared with Kedia d'Idjil. In brief, the present investigation offers comparisons of heavy metals contained in dust emissions as produced by iron ore mining. Results highlight the need for monitoring and controlling these emissions to reduce their environmental and human health implications.

### 3.3 Bacterial Analyzes

#### 3.3.1 Bacteria Quantification

The most probable number (5 tubes MPN) technique was used to obtain quantitative estimates of the bacteria in each sample. Quantification was achieved by serial dilutions of a bacterial culture, dividing the sample into replicates, followed by incubation and subsequent visual examination of each sample to determine growth. Table 2 presents the abundance of bacterial groups.

Table 2. Bacterial quantification results with a confidence interval of 95%.

Bacterial group	Types of samples	MPN g <sup>-1</sup>
Total anaerobic and microaerophilic bacteria	Guelb El Rhein	0
	Kedia d'Idjil	2100
Total aerobic bacteria	Guelb El Rhein	0
	Kedia d'Idjil	75

Although the initial quantification via the MPN method yielded zero counts for Guelb El Rhein dust (Table 2), this refers to the detection limit for directly cultivable total bacteria from the raw 1.5g sample. The subsequent identification of various *Staphylococcus* species (Table 3) was achieved by applying a thermal shock (63°C) and selective enrichment, which allowed for the isolation of specific strains that were either present in low concentrations or in a dormant state within the magnetite-rich matrix.

### 3.3.2 Bacterial Strains Isolation and Characterization

After subculturing the bacterial strains isolated from several prepared selective media and incubated at 37°C, the macroscopic study of the colonies obtained made it possible to differentiate several microbial strains according to their appearance (size, color, etc.). All strains were subcultured on nutrient agar and incubated at 37°C. Several subcultures were subsequently carried out to ensure their purity (by careful observation of the colonies formed after re-isolation and differential Gram staining). 15 pure gram-positive bacterial strains were thus selected for the rest of the present study.

### 3.3.3 Result of Gallery API Staph

The choice of the appropriate gallery API for the identification of isolates is made based on the results obtained from macroscopic, microscopic, and respiratory enzyme studies; this makes it possible to direct research towards certain bacterial genera.

After 24 hours of incubation at a temperature of 37°C, the results of the gallery API Staph (Table 3) were read and interpreted according to the reading table available on the technical sheet of the gallery Api Staph.

Table 3. Abundance (%) of bacterial isolated species tests performed by the API Staph gallery for the identification of strains in both types of iron ore.

Species	Kedia d'Idjil Dust (Hematite) (%)	Guelb El Rhien Dust (Magnetite) (%)
<i>Staphylococcus hominis</i>	11.92	10.96
<i>Staphylococcus capitis</i>	24.38	20.77
<i>Staphylococcus lentus</i>	0.00	22.76
<i>Staphylococcus epidermidis</i>	0.00	12.10
<i>Staphylococcus auricularis</i>	12.43	5.71
<i>Staphylococcus haemolyticus</i>	13.76	5.71
<i>Staphylococcus cohnii sub.urealyticum</i>	37.51	0.00
<i>Staphylococcus sciuri</i>	0.00	22.00

After confirming through the MPN test, we found that there is a significant amount of live bacteria in the dust emitted by SNIM.

Through an examination of the API Staph gallery, species were identified in the dust. It is remarkable, however, that all strains isolated as commensal species are also pathogenic staphylococci. The dust sample from Kedia d'Idjil, rich in hematite, also has a distinct bacterial community from the magnetite-rich Guelb El Rhien. The composition in percentages of different Staphylococci strains is, however, significantly divergent for both samples, which gives information on the intrinsic nature of each type of dust. Microorganisms The predominant microorganism in the dust of Kedia d'Idjil is *Staphylococcus capitis* (24.38%), followed by *Staphylococcus cohnii* sub. *urealyticum* (37.51%). Whereas the dust from Guelb El Rhien is characterized by a higher percentage of *Staphylococcus lentus* (22.76%) and *Staphylococcus sciuri* (22.00%). This variation in dominant bacteria indicates a site-specific diversity. Furthermore, Kedia d'Idjil dust is relatively evenly distributed and rich in *Staphylococcus capitis*, *Staphylococcus auricularis*, and *Staphylococcus haemolyticus*. By contrast, the spread of Guelb El Rhien dust is more diverse, with multiple strains such as *Staphylococcus epidermidis* and *Staphylococcus auricularis*. Another interesting feature is the relatively abundant occurrence of *Staphylococcus cohnii* sub. *Urealyticum* in Kedia d'Idjil dust, and it is not the case in Guelb El Rhien dust.

This difference raises questions about environmental factors unique to each area, like geology and climate, that may influence bacterial composition.

Comparing our results with similar studies could deepen our understanding of these findings. Future research might investigate whether these differences match patterns observed in other regions with different geological or climatic traits. Additionally, looking into the potential ecological and health effects of such variations in bacterial composition could help assess the environmental impact of these iron-rich dust types more thoroughly.

### **3.4 Recommendations to reduce the rate of dust emissions in SNIM**

#### **3.3.4 Causes of Failure**

This study aims to analyze the causes of the significant increase in dust emissions within the SNIM company and to propose appropriate solutions. Based on this analysis, it seeks to identify ways to reintroduce dust fallout into the production circuits.

These dust fallouts mainly correspond to iron production losses occurring at the final stage of processing. Their recovery and reintegration into the production cycle offer both economic benefits and a reduction in waste.

Table 4 presents the potential causes of dust emissions and their classification. These causes are grouped into five categories according to their origin within SNIM facilities.

Table 4. Causes of dust emissions in SNIM.

Material	Equipment	Method	Middle	Workforce
		Accidental walking		
Production quantity and delivery	Workshop maintenance	Inefficient air filtration system	Climatic condition	Lack of discipline Lack of training
Granulometry	Lack of means of recovery	Competence management	Air Currents	Lack of awareness
Humidity	Lack of staff	Corrective maintenance	Lack of cleaning	Lack of motivation
	Drop points		Clutter	

### 3.3.5 Criticality scale

The criticality index is calculated for each failure, from the combination of three criteria (Table 5), by multiplying their respective scores:

$$C = G \times F \times D$$

With:

- G: The severity of the consequences that the failure generates (index G);
- F: The frequency of occurrence of the failure (index F);
- D: The detectability of failure (index D).

Each of these criteria will be evaluated with a rating table established on 4 levels. Table 6 shows the criticality rating scale used.

Table 5. AMDEC rating grid.

Gravity (G)	
Note	Criteria
1	Indirect effect
2	Effect causing emission
3	Origin of the problem
4	Direct effect (dust emitter)
Frequency (F)	
Note	Criteria
1	Once a year
2	1 time/month
3	1 time/week

4	1 time/day
<b>Detectability (D)</b>	
Note	Criteria
1	Detection with appropriate indicator
2	Detection by an indirect indicator
3	Visual
4	Not detectable

Any criticality value over 24 will be leased to a significant aspect whose appearance will be addressed by the team.

The first level of criticality is based on the severity rating (assessment of the magnitude of the impact and its reversibility), while the second is based on repetition within a specified time interval.

The last level of criticality is based on dust emission indicators. Thus, for each criterion, a varying score between 1 and 4 will be assigned (the weighting factor for each criterion is 4).

The causes will be classified according to the scale of criticality. Thus, the causes and their criticality analyses will be presented at the beginning. Any cause with a criticality rating greater than 24 will be considered significant.

The values presented in Table 6 will make it possible to measure the causes of dust emission problems based on criticality.

Table 6. Criticality results with analysis.

Causes (aspects)	Analyses	G	F	D	C
Lack of staff, training, awareness, and motivation	A direct effect on production, daily and non-detectable.	4	4	4	64
Accidental walk	With an indirect effect on production, annually, and can be detected visually.	1	1	3	3
Lack of workshop maintenance	A direct effect on production, daily and non-detectable.	4	4	4	64
Lack of cleaning	With a direct effect on daily production, and detectable with an appropriate indicator.	4	4	1	16
Inefficient air filtration system	With a direct effect on daily production, and detectable with an appropriate indicator.	4	4	1	16
Footprint	A direct effect on production, daily and non-detectable.	4	4	4	64
The drop points	With a direct effect on production, annually, and detectable with an appropriate indicator.	4	1	1	4
Absence of means of recovery in time	A direct effect on production, daily, and non-detectable.	4	4	4	64

Presence of draft	With a direct effect on daily production, and detectable with an appropriate indicator.	4	4	1	16
-------------------	---	---	---	---	----

Due to the lack of history of these measurements, the threshold value of criticality was arbitrarily set at 24, which is a value resulting from a very serious cause, with an intermediate frequency and detected by an indirect indicator.

$$C = 4 \times 3 \times 2 = 24$$

To exploit the results of the AMDEC analysis, we proceeded as follows: technical solutions are proposed to reduce the criticality of the penalizing failure modes and to reach a maximum availability rate.

A maintenance policy based on the improvement actions of the AMDEC analysis is recommended, allowing the implementation of a preventive maintenance plan (Table 7).

Table 7. Results of significant criticalities with remedy.

Causes (aspects)	Criticality	Remedy
Lack of staff, training, awareness, and motivation	64	Plan, implement, and follow a training plan for employees
Lack of workshop maintenance		Revise the maintenance plan to promote preventive maintenance
Footprint		Expansion or investment of another line
Absence of means of recovery in time		Installation of a mining dome and acquisition of an industrial vacuum cleaner

#### 4. DISCUSSION

Dust deposition rates exhibited marked spatial variability across the sampling sites (Fig. 2), reflecting heterogeneous emission dynamics within and between the mining areas. During the exposure period, the Owens gauges collected 37,500 mg, 27,500 mg, and 49,700 mg of dust at stations a, b, and c, respectively, at the Guelb El Rhein mine, compared to 18,600 mg, 11,800 mg, and 14,800 mg at stations d, e, and f at the Kedia d'Idjil mine. The exceptionally high deposition rates recorded at Guelb El Rhein (38,045–50,480 mg/m<sup>2</sup>/day) significantly exceed the threshold for extremely polluted environments (>1000 mg/m<sup>2</sup>/day). These values reflect the strategic positioning of Owen gauges (Stations a, b, and c) in immediate proximity to the primary crushing and enrichment units of the Guelb 2 production circuit. These measurements represent source-point emissions under peak operational conditions rather than ambient background levels, explaining the several orders of magnitude difference from standard polluted environment thresholds.

These variations indicate that dust emissions are strongly influenced by local working conditions, equipment operation and maintenance, climatic parameters, and human activities.

Comparison of the measured values with reference thresholds revealed that dust emission rates at Guelb El Rhein significantly exceeded the limit for highly polluted areas ( $>1000 \text{ mg/m}^2/\text{day}$ ) and were substantially higher than those observed at Kedia d'Idjil and in the urban center of Zouérate. In contrast, dust deposition rates at the Kedia d'Idjil mine were close to the regulatory threshold and comparable to levels typically associated with livable environments. These differences suggest that operational constraints such as the need to halt production during equipment maintenance may contribute to elevated emissions and associated productivity losses.

X-ray fluorescence analysis confirmed the presence of silica dioxide in dust samples from both mining sites, with notably higher concentrations at Guelb El Rhein (Fig. 3). The toxicity of mineral dust, particularly crystalline silica, has been extensively documented (Fubini et al. 1999). Inhalation of silica-containing dust represents a major occupational health risk, as respirable particles can penetrate deep into the pulmonary region where gas exchange occurs (Roberge et al. 2004). The International Agency for Research on Cancer has classified inhaled crystalline silica (quartz and cristobalite) as a Group 1 human carcinogen (IARC 1997). However, its carcinogenic potential may vary depending on mineralogical characteristics, surface properties, particle morphology, and associated impurities (IARC 2012; UNICEM 2014).

Beyond chemical hazards, the microbiological analysis revealed a substantial presence of *Staphylococcus* species in the dust, highlighting an additional biological risk associated with mining emissions. Several studies have demonstrated that *Staphylococcus* spp. can exhibit high resistance to heavy metals such as copper, nickel, cobalt, and lead (Nieto et al. 1989; Sabry et al. 2008; Avilés et al. 1993), potentially due to selective pressure exerted by metal-rich environments. This resistance may be further enhanced by the widespread use of metal-based compounds in industrial and environmental applications (Hiramatsu et al. 1997).

Notably, *Staphylococcus* spp. have also been reported to possess biosorption capacities for heavy metals. Kumar et al. (2010) demonstrated up to 93% lead removal by *Staphylococcus* strains, while Rahman et al. (2019) reported strong lead-binding capacity in *Staphylococcus hominis* strain AMB-2. These findings suggest a dual role of *Staphylococcus* spp. as both indicators of environmental contamination and potential agents of bioremediation.

Marked differences in *Staphylococcus* community composition were observed between the two mining sites, reflecting site-specific environmental conditions. At Kedia d'Idjil, *Staphylococcus capitis* (24.38%) and *Staphylococcus cohnii*

subsp. *urealyticum* (37.51%) predominated, whereas dust from Guelb El Rhein was characterized by higher proportions of *Staphylococcus lentus* (22.76%) and *Staphylococcus sciuri* (22.00%). Several of these species are known opportunistic pathogens associated with bacteremia, endocarditis, urinary tract infections, and other severe clinical conditions (Wieser & Busse 2000; Meservey et al. 2020; Fan et al. 2020; Koksal et al. 2009).

The relatively homogeneous distribution of species in Kedia d'Idjil dust contrasts with the higher microbial diversity observed at Guelb El Rhein, suggesting that geological context, mineral composition, and operational practices may exert strong selective pressure on microbial communities. Furthermore, resistance to heavy metals and antibiotics has been reported in species such as *Staphylococcus epidermidis* and *Staphylococcus haemolyticus*, with co-selection mechanisms driven by environmental contamination (Sitthisak et al. 2005; Xue et al. 2015).

We hypothesize that the distinct bacterial communities observed dominated by *S. capitis* in the hematite-rich Kedia d'Idjil site and *S. lentus* in the magnetite-rich Guelb El Rhein site reflect selective pressures exerted by the specific mineralogical composition and associated heavy metal profiles of each environment. In metal-enriched mining settings, microorganisms often develop adaptive mechanisms that allow them to tolerate or transform toxic elements, including metal efflux systems and intracellular sequestration processes, as highlighted by Rajput et al. (2025). Although further mechanistic and statistical analyses are required to confirm this relationship, the observed site-specific microbial diversity suggests that the mineralogical characteristics of iron ores may act as a key driver shaping microbial assemblage structure in these mining environments.

Finally, the Failure Modes, Effects, and Criticality Analysis (FMECA) highlighted poor workshop maintenance, operational congestion, and delays in corrective measures as major contributing factors to dust emissions, with criticality indices exceeding 24. Preventive actions targeting these factors were therefore recommended to improve production efficiency, reduce emissions, and extend equipment lifespan.

## 5. CONCLUSIONS

Dust emissions along the production circuit of the Guelb El Rhein mine operated by the National Industrial and Mining Company have reached critical levels, posing serious environmental and occupational health risks. This study developed and implemented a comprehensive monitoring framework to quantify dust emissions, identify their sources, and assess both their chemical composition and associated bacterial load.

The results demonstrated that dust emission levels at Guelb El Rhein substantially exceed international safety thresholds (1000 mg/m<sup>2</sup>/day, AFNOR), rendering certain areas unsafe for personnel involved in production monitoring. In contrast, emissions at the Kedia d'Idjil mine remained closer to acceptable limits, highlighting the influence of site-specific operational and geological factors.

Chemical analyses confirmed the presence of silica and heavy metals in emitted dust, while microbiological investigations revealed a diverse assemblage of potentially pathogenic *Staphylococcus* species, underscoring the combined chemical and biological hazards associated with mining dust. These findings emphasize the need for integrated mitigation strategies addressing both particulate matter and microbial exposure.

To reduce dust emissions and associated risks, the implementation of preventive measures is strongly recommended, including:

- installation of enclosed mining domes to limit dust dispersion;
- deployment of conveyor belt recovery systems to recapture iron-rich dust;
- integration of air filtration and ventilation systems in enclosed workshops;
- installation of localized extraction hoods at material drop points to direct dust toward filtration units.

In addition to occupational exposure, gravity-driven deposition of particulate matter can lead to contamination of soils, vegetation, and water bodies, potentially causing habitat degradation and biodiversity loss if emissions are widespread and persistent. Overall, this study highlights the urgency of adopting sustainable dust management practices in mining environments to protect workers, surrounding ecosystems, and public health.

**Author Contributions:**

Conceptualization: Melainine Aillal and Olfa Ben Said; methodology: Hamouda Beyrem; software: Zeinebou Sidoumou; validation: Melainine Aillal, Olfa Ben Said, and Hamouda Beyrem; formal analysis: Melainine Aillal; investigation: Hamouda Beyrem; resources: Zeinebou Sidoumou; data curation: Melainine Aillal; writing—original draft preparation: Melainine Aillal; writing—review and editing: Olfa Ben Said and Hamouda Beyrem; visualization: Melainine Aillal; supervision: Olfa Ben Said; project administration: Zeinebou Sidoumou; funding acquisition: Olfa Ben Said. All authors have read and agreed to the published version of the manuscript.

**Funding:**

This research received no external funding.

**Institutional Review Board Statement:**

Not applicable.

**Informed Consent Statement:**

Not applicable.

**Acknowledgments:**

The authors thank all individuals and institutions who provided technical and administrative support for this study.

**Conflicts of Interest:**

The authors declare no conflicts of interest. The funders had no role in the design of the study; in the collection, analysis, or interpretation of data; in the writing of the manuscript; or in the decision to publish the results.

**6. REFERENCES**

1. Adamson, I., Prieditis, H. and Hedgecock, C., 2000. Zinc is the toxic factor in the lung response to an atmospheric particulate sample. *Toxicol Appl Pharmacol*, 166, pp.111–119.
2. Afnor, 2003. NF X43-014: Détermination des retombées atmosphériques totales – Échantillonnage, préparation des échantillons avant analyses, 32 p.
3. Aillal, M., Khazri, A., Al-Hoshani, N., Boufahja, F., Beyrem, H. and Lafdal, M.Y., 2023. Are iron ore microparticles toxic for the European clam *Ruditapes decussatus*? Response elements from biomarker activities and in silico modeling. *Saudi J Biol Sci*, 30, 103718.
4. Anthoine, D. and Humbert, J.C., 2007. *Atlas de Pathologie Thoracique*. Springer. doi:10.1007/978-2-287-48492-6
5. Antoine, C., 2012. Exposition aux poussières provenant d'une mine à ciel ouvert: évaluation des risques et biodisponibilité des métaux. Essai présenté au Centre Universitaire de Formation en Environnement, 87 p.
6. Aouissi, A., Fouzari, A. and Meziane, N., 2007. Qualité bactériologique de l'eau d'Oued Seybouse. Mémoire d'ingénieur. Université 8 Mai 1945 Guelma, 57 p.
7. Avilés, M., Codina, J.C., Pérez-García, A., Cazorla, F., Romero, P. and De Vicente, A., 1993. Occurrence of resistance to antibiotics and metals and of plasmids in bacterial strains isolated from marine environments. *Wat Sci Tech*, 27, pp.475–478.
8. Blanchon, V. and Penven, M., 2012. Jean Lefebvre Méditerranée Fos sur Mer (13): Compte rendu des mesures des retombées atmosphériques de poussières dans l'environnement autour de la future plate-forme multimodale. 19 p.
9. Boussahel, S., 2007. Analyse des retombées particulières aux alentours de la cimenterie d'Ain-El-Kebira. Mémoire de fin d'étude en vue de l'obtention du diplôme d'ingénieur d'état en écologie végétale et environnement, 88 p.
10. Brown, A.E. and Smith, H., 2015. *Benson's Microbiological Applications: Laboratory Manual in General Microbiology*, 13th ed. McGraw-Hill Higher Education, New York, 5 p.
11. Budillon, R., 2009. Carrière de Saint-Paul-lès-Romans. Règles techniques concernant les poussières, 15 p.
12. Chandrapati, S. and Williams, M.G., 2014. Comptes viables totaux | Nombre le plus probable (MPN). *Encyclopédie de Microbiologie Alimentaire*, pp.621–624.
13. Chen, H. and Zhang, J., 2022. Exploring the role of *Staphylococcus aureus* in inflammatory diseases. *Toxins*, 14(7), pp.464–464.
14. Debabza, M., 2015. Emergence en milieu hospitalier des bacilles Gram négatifs multirésistants aux antibiotiques: étude bactériologique et moléculaire. Thèse de doctorat d'état, Université Badji Mokhtar-Annaba, pp.5–65.
15. Eduard, W., Heederik, D., Duchaine, C. and Green, B.J., 2012. Bioaerosol exposure assessment in the workplace: the past, present and recent advances. *J Environ Monit*, 14, pp.334–339.
16. Elodie, G., Diane, L.B. and Fabrice, A., 2020. Rôle des particules dans la contamination en micropolluants des retombées atmosphériques. PIREN-Seine Phase 8 - Rapport 2020, p.9.
17. Embile Jr., R.F., Walder, I.F., Schuh, C. and Donatelli, J.L., 2018. Cu, Pb and Fe release from sulfide-containing tailings in seawater: results from laboratory simulation of submarine tailings disposal. *Mar Pollut Bull*, 137, pp.582–592.

18. Fan, Z., Yang, Y., Li, D. and Fei, Q., 2020. A rare lumbar pyogenic spondylodiscitis caused by *Staphylococcus caprae* with initial misdiagnosis: case report and literature review. *BMC Surg*, 20(1), pp.200–200.
19. Fubini, B., Zanetti, G., Altiglia, S., Tiozzo, R., Lison, D. and Safflotti, U., 1999. Relationship between surface properties and cellular responses to silica: studies with heat-treated cristobalite. *Chem Res Toxicol*, 12, pp.737–745.
20. Ha, E.T. and Heitner, J.F., 2021. *Staphylococcus auricularis* endocarditis: a rare cause of subacute prosthetic valve endocarditis with severe aortic stenosis. *Cureus*, 13(1).
21. Hariz, S., 2009. Etude critique du système de management environnemental au niveau des entreprises algériennes. Mémoire master en Hygiène et Sécurité Industrielle, 161 p.
22. Hassanvand, M.S., Naddafi, K., Faridi, S., Nabizadeh, R., Sowlat, M.H., Momeniha, F., Gholampour, A., Arhami, M., Kashani, H., Zare, A., Niazi, S., Rastkari, N., Nazmara, S., Ghani, M. and Yunesian, M., 2015. Characterization of PAHs and metals in indoor/outdoor PM10/PM2.5/PM1 in a retirement home and a school dormitory. *Sci Total Environ*, 527–528, pp.100–110.
23. Heederik, D. and Von Mutius, E., 2012. Does diversity of environmental microbial exposure matter for the occurrence of allergy and asthma? *J Allergy Clin Immunol*, 130, pp.44–50.
24. Jensen, H.J.H., Pedersen, J.E., Jorgensen, J., Skov Pedersen, K.D., Joensen, S.B., Iversen, E.G. and Sogaard, 2006. Determination of size distributions in nanosized powders by TEM, XRD, and SAXS. *J Exp Nanosci*, 1(3), pp.355–373.
25. Kumar, A., Bisht, B.S. and Joshi, V.D., 2010. Biosorption of heavy metals by four acclimated microbial species, *Bacillus* spp., *Pseudomonas* spp., *Staphylococcus* spp. and *Aspergillus niger*. *J Biol Environ Sci*, 4(12), pp.97–108.
26. López-García, I., Viñas, P., Campillo, N. and Hernández-Córdoba, M., 1995. Use of submicroliter-volume samples for extending the dynamic range of flow-injection flame atomic absorption spectrometry. *Anal Chim Acta*, 308, pp.85–95.
27. Ma, J., Chen, L., Guo, Y., Wu, Q., Yang, M., Wu, M. and Kannan, K., 2014. Phthalate diesters in airborne PM2.5 and PM10 in a suburban area of Shanghai: seasonal distribution and risk assessment. *Sci Total Environ*, 497–498, pp.467–474.
28. Manceau, A., Lanson, B. and Drits, V.A., 2002. Structure of heavy metal sorbed birnessite. Part III: results from powder and polarized extended X-ray absorption fine structure spectroscopy. *Geochim Cosmochim Acta*, 66, pp.2639–2663.
29. Meservey, A., Sullivan, A., Wu, C. and Lantos, P.M., 2020. *Staphylococcus sciuri* peritonitis in a patient on peritoneal dialysis. *Zoonoses Public Health*, 67(1), pp.93–95.
30. National Institute for Occupational Safety and Health, 1998. Childhood Agricultural Safety and Health Research; Notice of Availability of Funds for Fiscal Year. pp.3134–3138.
31. Nieto, J.J., Fernández-Castillo, R., Márquez, M.C., Ventosa, A., Quesada, E. and Ruiz-Berraquero, F., 1989. Survey of metal tolerance in moderately halophilic eubacteria. *Appl Environ Microbiol*, pp.2385–2390.
32. Nuzhat, J., Sajjad, H., Mohammad, V., Muhammad, Y., Rashid, I., Rana, R., Muhammad, Z. and Ambreen, A., 2022. Evaluation of the bioremediation potential of *Staphylococcus lentus* inoculations of plants as a promising strategy used to attenuate chromium toxicity. *Sustainability*, 14(20), pp.13056–13056.
33. Rahman, Z., Thomas, L. and Singh, V.P., 2019. Biosorption of heavy metals by a lead (Pb) resistant bacterium, *Staphylococcus hominis* strain AMB-2. *J Basic Microbiol*, 59(5), pp.477–486.
34. Rajput, P., Benjwal, S. and Pandey, R., 2025. A Comprehensive Review on the Role of Bioremediation in Heavy Metal Contamination. *Nature Environment & Pollution Technology*, 24. 10.46488/NEPT.2024.v24iS1.017
35. Rapilly, F., 1968. Les techniques de mycologie en pathologie végétale. *Ann Epiphyt*, 19 (n° hors série), 97 p.
36. Ron, J., 2006. X-ray techniques: overview. *Encyclopedia of Analytical Chemistry*, p.20.
37. Rouaiguia, M., 2010. Qualité microbiologique de l'eau de Oued Messida. Mémoire de master 2, Université 8 Mai 1945 Guelma, 78 p.

38. Sabry, S.A., Ghozlan, H.A. and Abou-Zeid, D.-M., 1997. Metal tolerance and antibiotic resistance patterns of a bacterial population isolated from sea water. *J Appl Microbiol*, 82(2), pp.245–252.
39. Sammut, M., 2007. Spéciation du cadmium, du plomb et du zinc dans les poussières d'émissions atmosphériques d'origine sidérurgique: approche de l'impact toxicologique des poussières. Thèse, Université Paul Cézanne, 254 p.
40. Simpson, S.L. and Spadaro, D.A., 2016. Bioavailability and chronic toxicity of metal sulfide minerals to benthic marine invertebrates: implications for deep sea exploration, mining and tailings disposal. *Environ Sci Technol*, 50, pp.4061–4070.
41. Sitthisak, S., Howieson, K., Amezola, C. and Jayaswal, R.K., 2005. Characterization of a multicopper oxidase gene from *Staphylococcus aureus*. *Appl Environ Microbiol*, 71, pp.5650–5653.
42. SNIM, 2022. Rapport annuel: un engagement durable et responsable. Société Nationale Industrielle et Minière, p.98.
43. Tecslult International Limited, 2009. *SNIM's Guelbs II Project, Mauritania – Environmental and Social Impact Assessment – Summary*. Préparé pour la Société Nationale Industrielle et Minière de Mauritanie, Nouadhibou: SMIM, 636 p.
44. Viegas, C., Fleming, G.T.A., Kadir, A., Almeida, B., Caetano, L.A., Quintal Gomes, A., et al., 2020. Occupational exposures to organic dust in Irish bakeries and a pizzeria restaurant. *Microorganisms*, 8, 118.
45. Winberry, W., 1999. Method IO-2.1 - Sampling of ambient air for total suspended particulate matter (SPM) and PM10 using high volume (HV) sampler (EPA/625/R-96/010a). Office of Research and Development U.S. Environmental Protection Agency, Cincinnati, 74 p.
46. Xue, H., Wu, Z., Li, L., Li, F., Wang, Y. and Zhao, Z., 2015. Coexistence of heavy metal and antibiotic resistance within a novel composite *Staphylococcal* cassette chromosome in a *Staphylococcus haemolyticus* isolate from bovine mastitis milk. *Antimicrob Agents Chemother*, 59(9), pp.5788–5792.
47. Yan, C., Leng, Y.L. and Wu, J.T., 2021. Quantitative microbial risk assessment for occupational health of temporary entrants and staffs equipped with various grade PPE and exposed to microbial bioaerosols in two WWTPs. *Int Arch Occup Environ Health*, 94, pp.1327–1343.